CULATION OF PARTIAL MOLAR VOLUME AND ITS COMPONENTS
FOR MOLECULAR DYNAMICS MODELS OF DILUTE SOLUTIONS

N. N. Medvedev,[1,2] V. P. Voloshin,[1] A. V. Kim,[1]
A. V. Anikeenko,[1] and A. Geiger[3]

This paper is a review of our recent computational studies of volumetric characteristics using computer models of dilute solutions. Partial molar volume (PMV) and its components are calculated for simple and complex molecules in water (methane, noble gases, surfactants, polypeptides). Advantages and disadvantages of various computational methods are discussed. It is proposed to use the Voronoi–Delaunay technique to determine the reasonable boundary between a solute molecule and solvent molecules and to identify the PMV components related to the molecule, the boundary layer, and the solvent. It is noted that the observed increase in PMV with temperature for large molecules is due to an increase in the volume of voids in the boundary layer, i.e., due to the "thermal volume." In this case, the solvent gives a negative contribution to the PMV. In contrast, for simple molecules (methane), the contribution from the solvent is positive and is the main factor in the increase in the PMV, which is associated with a specific change in water structure around a spherical hydrophobic particle outside the boundary layer. For surfactant molecules, the contribution from the solvent changes sign (from negative to positive) with increasing temperature.

INTRODUCTION

Molecular dynamics models provide solutions to many problems of the structure of solutions that cannot be solved by theory or experiment. Of great interest is to study the partial molar volume (PMV). This characteristic, on the one hand, is thermodynamic and is related to the other thermodynamic parameters. The PMV is defined as the change in the volume of the solution upon adding a solute (N_1) while maintaining the same volume of the solvent (N_2), temperature, and pressure:

$$V_{\mathrm{PMV}} = (\partial V / \partial N_1)_{T,P,N_2}.$$

According to thermodynamics, the PMV can be expressed, e.g., in terms of the derivative of the chemical potential with respect to pressure. In this aspect, the PMV is an extremely useful quantity to study the effect of pressure on the chemical reactions occurring in solutions, including the conformational transitions of the solute molecules. On the other hand,

the PMV is a geometric quantity — the volume that can be measured both experimentally and using molecular dynamics models of solutions.

In recent years there has been considerable interest in the PMV in molecular biology. The PMV for various biological molecules have been measured experimentally as a function of temperature and pressure, see, e.g., [1-9]. This helps to study the folding of proteins. However, to properly interpret these experiments, one must be able to identify the PMV components, i.e., the contributions due to the molecule itself and the surrounding water.

For infinitely dilute solutions, the PMV coincides with the apparent volume and is calculated for one solute molecule [10, 11]. Therefore, for such solutions, instead of the term PMV one sometimes uses the term (apparent) volume [12-15]. Below, for the sake of brevity, we will also use this term, i.e., instead of V_{PMV} we will write V_{app} everywhere. Thus, we emphasize that we are dealing with only one solute molecule, whereas the concept of PMV is defined for any concentrations.

Obviously, the value of V_{app} depends on the size of the solute molecule and also on the changes it causes in the solvent. Thus, it can be divided into two main parts — the contribution of the molecule V_{int} and the contribution of the solvent ΔV:

$$V_{app} = V_{int} + \Delta V. \tag{1}$$

The *intrinsic* volume V_{int} obviously includes the volume of the molecule (van der Waals volume with internal cavities) and a part of the empty space from the boundary region. Intermolecular voids are always present in solutions and some part of this empty volume is naturally associated with the solute molecule. The *contribution of the solvent* ΔV refers to the entire solvent. In this case, it is understood as the difference between the volume of the solvent in the solution ("perturbed" by the solute molecule) and the same volume of pure solvent [14]. It does not matter in this case which interactions with the solute molecule have caused this perturbation. In addition, the contribution ΔV contains the universal thermodynamic term $k\beta_T T$, see below.

Many papers, see, e.g., surveys [1, 16], use a somewhat different representation of the apparent volume taken from earlier studies [17, 18] based on SPT theory [19, 20]:

$$V_{app} = V_M + V_T + V_I + k\beta_T T. \tag{2}$$

Here V_M is the volume of the solute molecule, by which is usually meant the *molecular* volume, i.e., as is common in molecular biology, the van der Waals volume of the molecule with internal voids [21-24]. Thus, this term is the trivial solvent-excluded volume; i.e., the volume forbidden for solvent molecules.

V_T is the so-called *thermal* volume. It is caused by another universal factor which contributes to the apparent volume. This additional void volume, as stated in [25] is "due to the mutual vibrations of solute and solvent molecules, as well as structural, packing and steric effects." According to SPT theory, the true excluded volume associated with the solute molecule is given by the sum $V_M + V_T$ and corresponds to the volume of the cavity V_C that needs to be created to accommodate the solute molecule. The volume V_T is represented by a layer of certain thickness δ around the molecule [17, 18, 25]. However, this representation of the thermal volume is not universally accepted. The additional voids discussed are associated with the entire boundary region between the molecule and the solvent, so that it always remains unclear what part of this volume should be assigned to the layer δ. Furthermore, in [16, 26], the thermal volume is associated not with the molecule, but with the solvent, although its physical nature is treated similarly: it "results from thermally induced molecular fluctuations between the solute and solvent and is considered as average empty space around the solute due to imperfect packing of solvent." [16].

V_I is the volume due to molecule–water *interactions* other than the above-mentioned steric effects generating the thermal volume. Usually, by this volume is meant the result of the exposure of water to electric charges and dipoles present on the solute molecule [1, 18, 26].

$k\beta_T T$ is a universal thermodynamic addition, which is believed to be independent of the solute molecule and is determined only by the temperature T and the isothermal compressibility of the solvent β_T. It reflects the fact that the solute molecule contributes its translational degrees of freedom to the system, which contribute to the apparent volume, in addition

to the excluded volume of the solute molecule [27-30]. In the case of rarefied gases, this contribution is decisive. Indeed, as can be seen from the ideal gas law $PV = NkT$, the addition of one more molecule to the system (transition to $N + 1$ molecules) causes a change in the volume of the system by a finite value $V_{app} = kT/P$. In this case, the size of the molecule itself can be arbitrarily small. In general, this thermodynamic contribution is expressed in terms of fluctuations of the volume associated with a given number of solvent molecules, see, e.g. [30]. For dense solutions, however, this contribution is small compared to the apparent volume of the solute molecule, and is usually neglected. Even for a molecule such as methane, its inclusion does not contribute significantly to the interpretation of volumetric characteristics in an aqueous solution, see below.

Note that the decompositions of the apparent volume in formulas (1) and (2) are based on different considerations. Thus, the components V_{int} and ΔV in formula (1) are associated with regions of space: the region related to the solute molecule and the region related to the solvent — irrespective of the details of the interaction between the molecule and the solvent. In contrast, in formula (2), the terms V_T and V_I are defined as the result of the physical effect of the molecule on the solvent, and their geometric identity is not obvious. Thus, the dipole moment of the molecule can lead to a change in water structure outside the boundary region, i.e., contributes to V_I. However, it necessarily affects the nearest water molecules, i.e., also makes a contribution to V_T.

Most theoretical studies of PMVs focus on calculating the PMV for a particular molecule or class of molecules. Typically, use is made of the idea that the PMV of a large molecule can be calculated as the sum of the PMV of its atoms (molecular groups) is used [7, 18, 31].This approach works, at least for linear molecules, including polypeptides. For example, the apparent volume of a hIAPP molecule calculated from the known apparent volume of its constituent amino acids using the procedure described in [7] is in good agreement with the apparent volume obtained by molecular dynamics simulations [15] (Fig. 1). Another interesting approach to the prediction of the apparent volume is based on RISM theory [32, 33]. Using this theory, it is possible to calculate the partial functions of the radial distribution of water relative to the solvent atoms. Then, the Kirkwood–Buff approach is used in which the PMV is expressed in terms of the integral of these functions [16, 4, 35].

In contrast to these studies, we do not aim to predict the value of PMV for any molecules. Our task is to calculate the apparent volume and its components for computer models of solutions. At present, the molecular dynamics method is widely used to model solutions, including for PMV calculations, see e.g., [2, 14, 15, 25, 36-38]. However, there are still some problems to be solved to obtain reliable results. In this paper, we discuss the methods used in such calculations considering as an example infinitely dilute aqueous solutions of both complex and simple molecules.
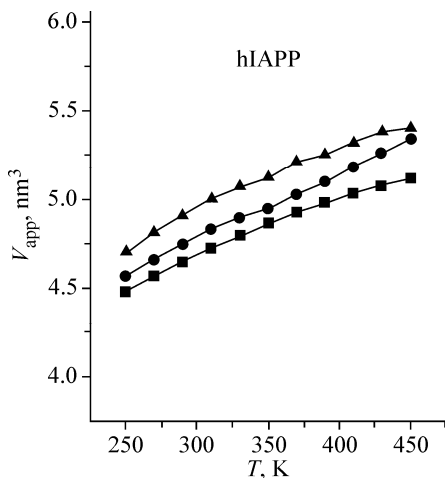
CALCULATION OF THE APPARENT VOLUME

Our models contain only one molecule of solute in simulation box surrounded by a large number of molecules of the solvent (water). Periodic boundary conditions reproduce the solute molecule in each periodic image of the simulation box, but it never approaches its images and the interaction between them is considered negligibly small. In this sense, our models are infinitely dilute solutions.

From the point of view of the experimenter, the apparent volume of the solute molecule V_{app} is defined as the difference between the volumes of the solution and the corresponding amount of the pure solvent. According to a popular legend, Archimedes found the volume of a gold crown assuming that it is equal to the volume of water displaced. However, for the molecule, the observed increase in the volume of the solution is not its "true" volume. The "apparent" volume of the molecule is measured which contains contributions from the molecule itself and from the solvent. In the case of molecular dynamics simulations, the apparent volume of the solute molecule corresponds to the difference between the average volumes of simulation boxes with the solution and pure solvent:

$$V_{app} = \left\langle V_{box}^{Solution} \right\rangle - \left\langle V_{box}^{Solvent} \right\rangle. \tag{3}$$

Both models should be obtained for the same pressure and temperature (in the NPT ensemble) and the same number of solvent molecules in the solution and in the pure solvent. This method of calculation corresponds to the definition of the apparent

Fig. 1. Apparent volume of a hIAPP molecule in water calculated for a molecular dynamics model of the solution using different methods [36, 40]. The upper curve (triangles), taken from [36], was obtained by the *direct* method. The middle curve (circles), taken from [15], was obtained by the *combined method*, see the text. The lower curve, taken from [7], was obtained by an empirical method based on the summation of the contributions from the individual amino acids.
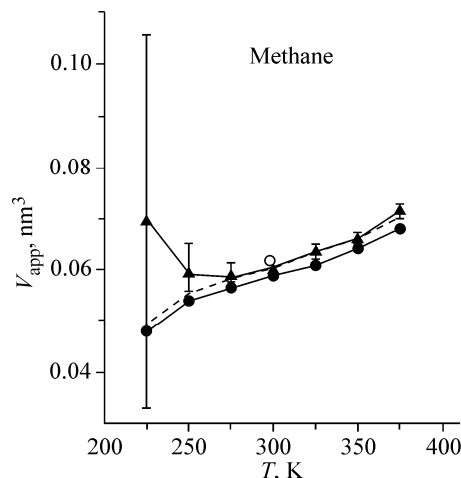
Fig. 2. Apparent volume of a methane molecule in water calculated by different methods. The upper curve (triangles) was obtained by the direct method. Dotted curve was obtained by a local (combined) method. The lower curve (circles) was obtained by the combined method ignoring the term $k\beta_T T$. The empty circle shows an experimental value of the apparent volume of methane at 300 K [41].

volume and is therefore called *direct*, as opposed to the other methods that use only the local the molecule and will be called *local,* see below.

DIRECT METHOD

In this case, the apparent volume is calculated by formula (3). Although here we proceed according to the definition, this method should be used with caution, since in some situations, it is not accurate enough. This is due to the fact that the unknown quantity V_{app} is a small part of the volume of the simulation box is calculated as the difference of large values, each of which is calculated with a certain error. Moskalev [39] calculated the average density of water in a molecular dynamic model as a function of the averaging time. It has been shown that, besides the usual fluctuations of the average volume of the simulation box (in the *NPT* ensemble) at picosecond times (about 1%), small volume variations remain (of the order 0.1%) after averaging over large intervals of hundreds or even thousands of picoseconds. They may have a statistical nature as being the result of averaging the fluctuating quantity over a finite interval, or they may be the result of a long relaxation of some structural fluctuations arising and decaying during modeling of the liquid phase. In any case, such small deviations are usually neglected, but they can appear in the calculation of the apparent volume. For example, if the apparent volume of a molecule is one-hundredth of the volume of the simulation box $V_{app} \approx 10^{-2} \cdot V_{box}^{Solvent}$ it is easy to see that an error of 0.1% in the volume of the simulation box will lead to an error of 10% in calculating the apparent volume. This is a large error, especially if we want to explore the components of the apparent volume.

Thus, if the volume of the box is substantially greater than V_{app}, a negligible uncertainty in finding the average volume of the box leads to a significant error of the desired quantity. Note that for the solution models considered below, the value of V_{app} is about 1/70 of the volume of simulation box for a hIAPP molecule, 1/200 for methane, and 1/300 for a C_8E_6 molecule.

We emphasize that when using the direct method, one should perform a special modeling of the pure solvent. Here it is important to use appropriate thermodynamic conditions (temperature and pressure) and simulation parameters (interatomic interaction).

Fig. 1 shows the data of [36] for the apparent volume of hIAPP polypeptide calculated by the direct method. It is evident that they are qualitatively consistent with the results obtained by other methods for the same models [15]. There is a similar increase with temperature, although there is a constant shift of the curves within 10% of the value of the volume itself. Unfortunately, in [36], details of the calculation are not described; in particular, it is not clear how the volume of the simulation box with the pure solvent was determined, and with what accuracy. Experimental values of apparent volume of this molecule are unknown.

Fig. 2 compares the apparent volume of a methane molecule in water calculated by different methods [42]. TIP4P/2005 water was used [43], and the methane molecule was described by a Lennard-Jones particle for which the parameters of methane–water interaction were taken from [38]. The solution consisted of a single methane molecule surrounded by 360 water molecules. Simulation parameters were taken from [44]. The characteristic volume of the simulation box was varied from $10.8\,\text{nm}^3$ to $11.3\,\text{nm}^3$ in the temperature range studied. The average volumes of the boxes were calculated by averaging over 50 ns for each temperature. The results of the calculation by the direct method by formula (3) (shown by triangles in the figure) are in very good agreement with those obtained by the combined method (dotted curve) discussed below for all temperatures, except for the lowest ones (region of supercooled water). The vertical lines in Fig. 2 show the error of the calculation of the apparent volume estimated by block averaging over the entire trajectory. It can be seen that at high temperatures, the error is small, and at low temperatures, it becomes large. This demonstrates the weakness of the direct method, discussed above. Large errors at low temperatures are attributed to the fact that the modeling and averaging over 50 ns are not sufficient to obtain reliable average values of the volume of the boxes for these temperatures.

Fig. 2 also shows the contribution of the thermodynamic term $k\beta_T T$ to the apparent volume. The direct method uses a molecular dynamic model of solutions which simulates real systems and therefore naturally contains this contribution. Local methods do not take into account the motion of the molecule itself in the solution, so that the term $k\beta_T T$ has to be introduced additionally. The dotted curve is obtained taking into account this term, and the lower curve (circles) is obtained without considering this term. It is indeed small (of the order of $0.002\,\text{nm}^3$) and changes only slightly in the temperature range considered. However, for the methane molecule, this value is about 5% of the apparent volume and, as we see, must be taken into account. As a result, there is very good agreement between the values of the apparent volume calculated by different methods, as well as with the experimental value [41]. For large molecules, this thermodynamic contribution is, of course, negligible.

Calculation of the apparent volume of a methane molecule by the direct method was also performed by Ashbaugh et al. [38]. The authors used 400 water molecules in the simulation box and simulated the solution for 50 ns and pure water for 100 ns at $T = 300$ K. The resulting calculated value of $37.1\,\text{cm}^3/\text{mol}$ is also in very good agreement with the experimental value of $37.14\,\text{cm}^3/\text{mol}$ (indicated by an empty circle in Fig. 2, after conversion to cubic nanometers).

Thus, the direct method is appropriate for the calculation of the apparent volume, but to provide reliable results, it requires a double simulation (of the solution and solvent) and careful averaging of the volumes of the simulation boxes.

LOCAL APPROACHES

Obviously, the solute molecule perturbs the surrounding water only in a certain neighborhood rather than over the entire solution. We will call this region the *hydration* (*solvation*) shell of the molecule in solution. Typically, it covers no more than 2-3 molecular layers, after which the water structure is not different from that of pure water. In particular, Pal et al. [45], analyzing femtosecond fluorescence experiments, concluded that beyond 7 Å from the surface of the biomolecule, water can be considered unperturbed.
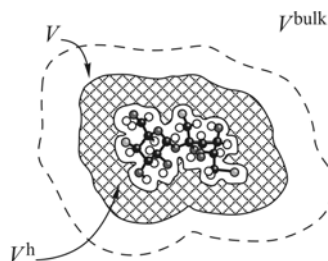
Fig 3. Illustration of the region V around a solute molecule for calculation of the apparent volume by the local method. The boundary of this region (dashed curve) should pass outside the hydration shell V^h (gray region around the molecule).

Thus, in calculating the apparent volume, it is not necessary to consider all water in the simulation box, but it is sufficient to consider only the neighborhood of the molecule. Therefore, instead of (3), it is proposed to use the expression

$$V_{app} = V - N / \rho_0 + k\beta_T T, \tag{4}$$

where V denotes some volume around the solute molecule which completely includes both the molecule itself and its hydration shell; N is the number of solvent molecules in the volume V; ρ_0 is the density of pure water at the same temperature and pressure. The term $k\beta_T T$, as noted above, must be added because the volume V and the number of water molecules N in this volume around the solute molecule are always examined without considering its motion in the solution, i.e. the molecule is assumed to be "fixed" and its translational degrees of freedom are not taken into account [29, 30].

Note that the region V in formula (4) can be rather arbitrary (Fig. 3). It does not matter where and how to draw its boundary, if only it lies entirely in bulk water. Indeed, any additional volume outside the hydration shell is fully compensated by the second term on the right side of formula (4) since, in this case, the number of water molecules N increases, on average, accordingly.

Since the outer boundary of the hydration shell is not known in advance, the boundary of the volume V should always be chosen with a margin. Below we discuss different methods of working with formula (4).

Note that formula (4) is seemingly transformed into formula (3) as the volume V tends to the volume of the entire simulation box. However, it is not correct to talk about this transformation because the physical content of these formulas is different. In formula (3), we used independent "vessels," each of which contained a liquid in thermodynamic equilibrium, whereas in formula (4), we consider the environment "tied" to the solute molecule.

Note that in the case of a spherical solute molecule, formula (4) reduces to the well-known Kirkwood—Buff formula for the calculation of the apparent volume [16, 25, 27, 28]:

$$V_{app} = -G + k\beta_T T. \tag{5}$$

G denotes the Kirkwood–Buff integral:

$$G = 4\pi \int (\rho(r) / \rho_0 - 1) r^2 dr, \tag{6}$$

where $\rho(r)$ is a function of the radial density distribution of water around the solute molecule; ρ_0 is its asymptotic value, i.e., the value for pure water. In formula (6), the range of integration is from zero to infinity, but in the analysis of models, the integration has to be restricted to a finite value for the upper limit. As discussed in [29, 46], this value of R can be chosen such that the integral $G(R)$ will be equal to its asymptotic value. Recall that function $G(R)$ has oscillations which are especially pronounced for simple solute molecules [29, 42, 46]; however, several distinct oscillation can also be seen around

complex molecules, see below. The volume V in formula (4) is represented by a sphere of radius R and arises from the second term in the integrand of (6), and the term N/ρ_0 is obviously obtained from the integration of the first term.

The Kirkwood–Buff approach is useful when it is possible to obtain somehow the function $\rho(r)$, e.g., by using RISM theory, after which the calculation of integral (6) is not difficult (see e.g., a review [16]). However, when working with computer models where the coordinates of all the atoms are known, one can immediately use the general formula (4), especially if the solute molecule has a complex shape.

We emphasize that formula (4) gives a rigorous definition of the apparent volume, as well as formula (3). It should only be remembered that the solution is assumed to be infinitely diluted. Only in this case does the calculated quantity in formula (4) represent the partial molar volume. There are still some questions about the term $k\beta_T T$ in the case of polyatomic solute molecules, where the internal degrees of freedom of the molecule must be somehow taken into account [47]. However, this problem is usually ignored because the thermodynamic contribution can be safely neglected for large molecules.

The Kirkwood–Buff formula (5) was derived based on statistical physics. However, it was also obtained assuming an infinitely dilute solution. The Kirkwood–Buff formalism requires that the integration in formula (6) be carried out from zero to infinity. From a physical point of view, this is redundant since the effect of the solute molecule occurs only at finite distances. From a theoretical point of view, it is necessary to take into account the difference in the asymptotic behavior of $\rho(r)$ in different ensembles (*NPT* and *NVT*), because of which the integration to infinity leads to different contributions to integral (6). This aspect of the theory is considered in [29, 46].

Traditional method. As a parameter for the selection of the volume V in formula (4), we use the distance R from the molecule:

$$V_{\mathrm{app}}(R)=V(R)-N(R)/\rho_0. \tag{7}$$

Here and below, we will not write out the universal term $k\beta_T T$ present in (4).

In general, working with molecules of arbitrary shape, it is convenient to measure the distance from a molecule from its surface. For a spherical molecule of radius R_{m}, the volume $V(R)$ is determined as the volume of a sphere of radius $(R + R_{\mathrm{m}})$, and the number $N(R)$ is the number of water molecules whose centers lie within the sphere. As the radius R_{m} we propose to use the quantity specified by the Lennard-Jones interaction potential used in the creation of of the model, i.e., $\sigma_{11}/2$ (or $(2\sigma_{12} - \sigma_{22})/2$ if, instead of σ_{11}, the cross-interaction parameter σ_{12} between the solute molecule and a molecule of water is specified, as is done in [38]). In our experience, this approach gives reasonable results (see Fig. 2). Note that the determination of the radius for an atom has always been and remains an open question to be specifically discussed for each specific problem.

For a molecule consisting of many atoms, the distance R defines a surface equidistant from the molecule. In molecular biology, there is the notion of the solvent accessible surface (SAS), which is separated from the molecule by a distance equal to the radius of a water molecule (usually 1.4 Å) [21, 24]. However, in our case, the distance R can be arbitrary, and quite large.

Calculation of the volume $V(R)$ within this surface is a difficult geometric problem. It reduces to finding the volume of a union of spheres of different radii, where the spheres are centered on the solute atoms and have radii equal to $R + R_{\mathrm{a}}$, where R_{a} is the radius of the corresponding atom (Fig. 4).

There are different ways to solve this problem using both numerical and analytical approaches in which formulas for calculating the multiple overlaps of the spheres are written explicitly. Recently, a new method has been proposed based on a Voronoi radical partition, which proved easier to implement and more stable when working with large molecules (for more details, see [49, 50]). In our work, we use the algorithm implemented in [49]. It is not difficult to find $N(R)$ for polyatomic molecules. As in the case of a spherical molecule, it is sufficient to select those water molecules whose centers are within the distance R. Note that for $R = 0$, we determine the van der Waals volume of the molecule, i.e., the volume of the union of atoms that form the molecule [21, 23]; see the lower horizontal dot-dashed curve in Figs. 5 and 6.
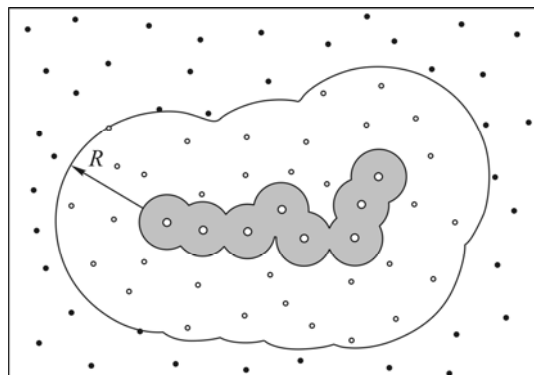
Fig. 4. Region $V(R)$ around a polyatomic solute molecule. The surface of this region is at a distance R from the molecule. Dots show the centers of solvent molecules.
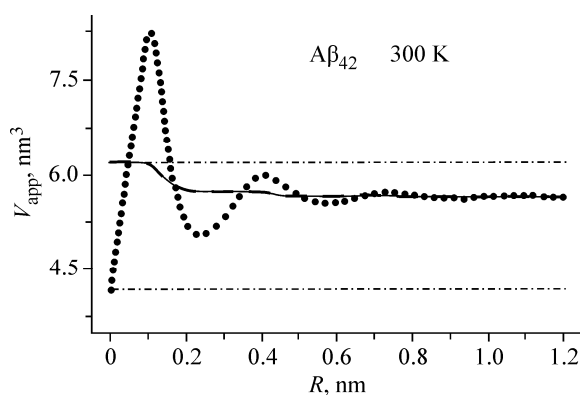
Fig. 5. Profile of the apparent volume of the $A\beta_{42}$ molecule calculated by formula (7) using the traditional method (dotted curve) and by formula (9) using the combined method (solid curve), taken from [15]. The lower horizontal dashed-dotted curve corresponds to the van der Waals volume of the molecule. The upper dot-dashed curve shows the Voronoi volume of the molecule in the solution, see the text.
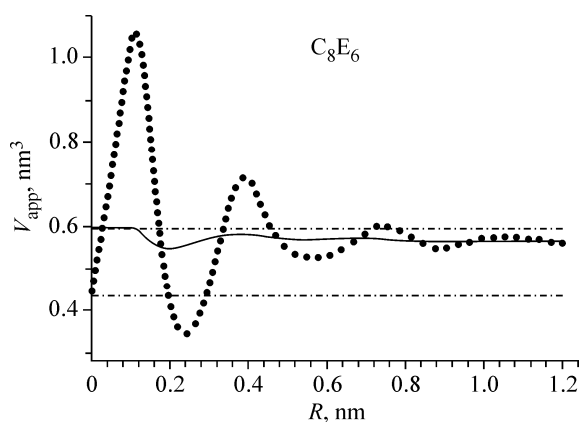

Fig. 6. Profile of the apparent volume of the C_8E_6 molecule calculated by formula (7) using the traditional method (dotted curve) and (9) and the combined method (solid curve), taken from [51].

In Figs. 5 and 6, the dotted curves show the dependences $V_{app}(R)$ calculated by the traditional method for molecular dynamics models of aqueous solutions of the polypeptide $A\beta_{42}$ [14], and the C_8E_6 amphiphilic molecule [51]. A characteristic feature of these curves is large oscillations of the functions. Deviations from the asymptotic value are observed even at large distances R of about 1 nm, and the smaller the molecule, the greater the relative deviation of the oscillation amplitudes from the asymptotic value. For the inert molecules of noble gases and methane, clear deviations are seen up to $R = 2$ nm [42, 46].

Note that the oscillations of the apparent volume profile should not be attributed only to the influence of the molecule on the surrounding water molecules. They are mainly associated with the intrinsic structure of the solvent and are due to oscillations of the function $\rho(r)$. The behavior of $\rho(r)$ reflects the three-dimensional structure of water as a function of the distance from the solute molecule to water molecules, just as the pair correlation function $g(r)$ reflects the three-dimensional structure of water as a function of the distance between water molecules. Figure 7 shows the water density distributions $\rho(r)$ around molecules of hIAPP, $A\beta_{42}$ and C_8E_6. It is seen that they are very similar, especially for the polypeptides. The differences in the first maximum are due to the specifics in the boundary regions of the different molecules. Similarity of the curves indicates that they are of the same nature, i.e., reflect the water structure in the solution.
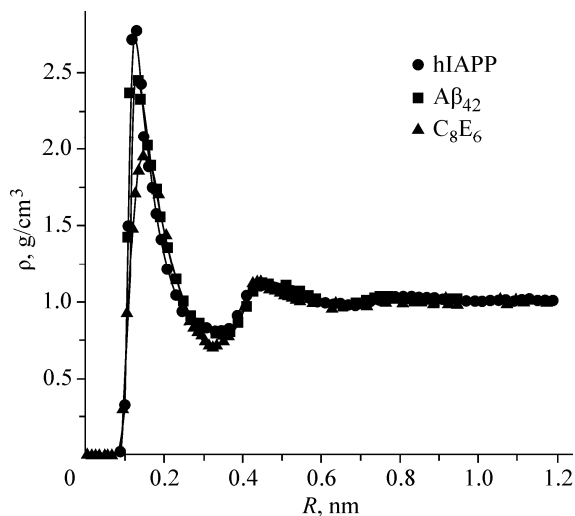
Fig. 7. Water density distribution functions $\rho(r)$ around polypeptides hIAPP and Aβ_{42} [15], and a C$_8$E$_6$ molecule. The curve for C$_8$E$_6$ is slightly shifted to show the good agreement after the first maximum.

Fig. 8. Region $V(R)$ around a solute molecule for calculation of the apparent volume by the combined method. The surface of this region is at distance R from the molecule (as in Fig. 4), and the volume is determined by the sum of the volumes of the Voronoi regions of all the atoms lying in this region: associated with the solute molecule (colored dark grey) and to the solvent (colored white).

It is clear that the observed oscillations of the profile of $V_{app}(R)$ can lead to significant errors in evaluating the asymptotic value of V_{app}. For example, choosing the boundary R for the hydration shell from the extrema or nodes of the function $\rho(r)$, as is sometimes done [14], we obtain a value of the apparent volume different from the asymptotic value, and the difference can be 10% or more if the boundary is chosen within the second maximum $\rho(r)$ (cf. Fig. 7 with Figs. 5 and 6).

Thus, the traditional method requires the calculation of the profile of $V_{app}(R)$ to sufficiently large distances R. Note that this is also true for the approach in which the Kirkwood–Buff integral G is calculated. However, increasing R again leads to the problem of the accuracy in determining the average difference of fluctuating large quantities since, in this case, the desired volume $V_{app}(R)$ becomes small compared to the volume $V(R)$ used, see above.

Combined method. Here, as in the traditional method, the region around the molecule is isolated by a predetermined distance R, Fig. 8. However, the volume $V(R)$ is calculated differently, namely as the sum of the volumes of the Voronoi regions of all atoms whose centers lie in the specified region. Thus,
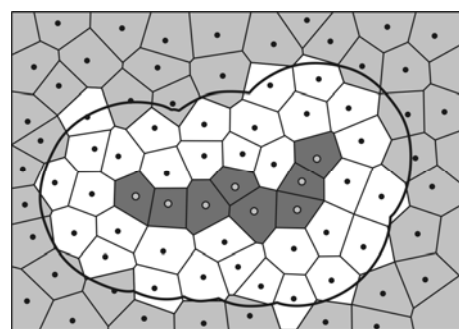
$$V(R) = \sum v_i. \tag{8}$$

The sum $\sum v_i$ can be separated into the sum over $N(R)$ of the solvent molecules $\sum v_s$ and the sum over all M atoms of the molecule $\sum v_m$. However, when calculating the apparent volume, we do not distinguish between these components, and simply sum the volumes of all atoms whose centers are within the shell R. Here we have avoided the difficult problem of calculating the volume within the complex R-shell, which has to be solved in the traditional method. However, another nontrivial problem arises: calculation of the Voronoi regions. Fortunately, it is also now resolved, and there are a large number of effective programs for their calculation, see, e.g., [52]. Recall that the Voronoi regions are cells of the *Voronoi partition*, which divides the space between the atoms without overlaps and gaps [53, 54].

Thus, using notation (8), formula (7) is converted to

$$V_{app}(R) = \sum v_i - N(R)/\rho_0. \tag{9}$$

An important advantage of this approach is that the profile of V_{app} now does not contain the unwanted oscillations observed in the traditional method (see the solid curves in Figs. 5 and 6). The reduction of the oscillations is due to the fact that the solvent molecules are now taken into account along with their volumes. Indeed, in the traditional method, the increment of R by a value ΔR causes a monotonic increase in $V(R)$ by a value of $4\pi R^2 \Delta R$, whereas the change in $N(R)$ depends, in addition, on the current value of the function $\rho(R)$. Now, however, with an increase in R, the first and second

terms on the right side of formula (9) change simultaneously (the volume $V(R)$ depends on the number $N(R)$), so that oscillations of the function $\rho(r)$ practically do not appear.

Note that both methods give the same value of the asymptotics $V_{app}(R)$ (Figs. 5 and 6). Now, however, it is achieved at much smaller distances. This eliminates the above-mentioned complexities of the traditional method.

One might reasonably ask, which method of calculating the volume $V(R)$ is more appropriate? In the first case, one considers the volume within a given R-surface, which has a clear geometric meaning. However, working with computer models of molecular systems, we can argue otherwise. We have identified a region of space which contains a certain amount of atoms. The volume of this region can be assumed to be the spatial volume associated (assigned) to these atoms. This situation is implemented using the Voronoi regions.

In view of the marked advantage of the combined method, we have chosen this method for our study, rather than the traditional method. However, there is one more method — the *method of Voronoi shells* [15], which is different from the two methods considered above. In this method, the hydration shell is identified without any additional parameter R, which is a definite advantage. However, there are some difficulties involved in working with a discrete Voronoi tessellation. In mathematics, it is known that the average volume of a cluster of adjacent cells of a tessellation is different from the intuitively expected value — the product of the number of cells in the cluster by the average volume of the cell across the tessellation. This fact is a consequence of the correlation between the cell volume and the number of its neighbors in the tessellation. Accounting for this fact requires some extra effort [15, 55]. Using the combined method, we avoid this problem, although it also uses Voronoi cells. In the combined method, Voronoi cells are selected based on their distance from the molecule, i.e., without the use of the topological connectivity of cells. As a result of this, the indicated correlation is practically not observed.

So, we believe that the combined method is the easiest and most reliable method for calculating the apparent volume.

CALCULATION OF THE COMPONENTS OF THE APPARENT VOLUME

The separation of the apparent volume into the components is always conditional. Decomposition into different components can be performed in both formula (1) and formula (2). However, in any case, there is the problem of determining the boundaries between the regions. When using formula (1), in is necessary to determine the boundary between the solute molecule and the solvent. Note that the solvent excluded surface (SES) and the solvent accessible surface (SAS) [21-24], which are well-known in molecular biology, are not suitable for this role. In the first case, allowance is not made for the intermolecular voids present in the solution, part of whose volume must be assigned to the solute molecule, and in the case of SAS, a too wide region around the solute molecule that includes parts of solvent molecules is considered. Formula (2) does not provide for spatial separation of the contribution of the thermal contribution V_T and the contribution due to the interaction V_I. However, in this case, the question of the boundary region between the solute molecule and the solution is still to be solved. For this region it is also necessary to define the boundaries, both internal and external.

The quantitative boundaries can be determined using Voronoi–Delaunay methods [53, 54]. This general geometric approach is widely used for the analysis of models where the coordinates (radii) of each atom are known. It is used to characterize the structure (relative position of atoms), as well as to distinguish and examine intermolecular voids. However, it should be remembered that there are different types of Voronoi–Delaunay partition. They differ in the how the distance from a point in space to an atom is measured. In principle, there may be different ways to measure the distance [53], but for physical applications, three types are of interest: *classic, radical* (*power*) (P-partition), *and additive-weighted* (S-partition), Fig. 9.

In the first case, the atoms are represented by points (their centers), i.e., we deal with a system of discrete points. It is with these systems that the founders of the method worked [56, 57]. In this case, the Voronoi regions are polyhedra, i.e., have
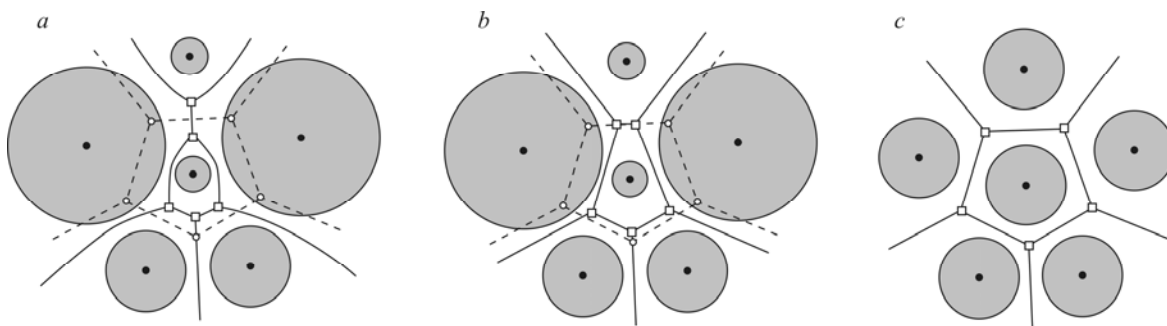
Fig. 9. Illustration of Voronoi regions of different types constructed for the central atom: S-region (solid curve) and classical (dashed curve) (*a*); P-region (solid curves) and the classical region (dotted curve) (*b*); in the case of atoms of the same size, all types of Voronoi regions are the same (*c*).

flat faces. If the size of the atom is not important, it is reasonable to use the classical partition since it is easier to calculate and analyze.

If interatomic voids are investigated, it is necessary to consider the size of the atoms. Here, one should use S-partition which defines Voronoi regions relative to the surfaces of atoms. Points of the Voronoi S-region of a given atom are closer to *the surface* of this atom than to *the surfaces* of other atoms of the system. It has a clear physical meaning, but its calculation and analysis is more complicated because the faces of the Voronoi S-regions are not flat in general. Nevertheless, methods for constructing this partition are currently developed and successfully used in the analysis of intermolecular voids [58-61]. An unsolved mathematical problem here is the calculation of the volumes of Voronoi S-regions. An analytical formula for its calculation is still unknown. Therefore, it is necessary to use numerical methods, which are inefficient when dealing with large molecular systems, especially where averaging over a large number of configurations of the molecular dynamics model is required. This problem can be overcome by using the radical partition.

P-partition takes into account the radii of atoms, but, perhaps, not in a "physical" way. Here the distance from a point in space to an atom (sphere) is measured along the tangent to its surface (in mathematics, this distance is called the power of the point). Of course, the Voronoi P-region differs somewhat from the S-region for the same atom in the same environment (Fig. 9*a* and *b*). This difference is usually small if the size of the atoms do not differ greatly (as in molecular systems), and it disappears if the atoms become identical (Fig. 9*c*). It is important that the P-regions are polyhedra, as in the classical case; i.e., they are convenient for calculation and analysis. (By the way, the letter P is used to denote the Voronoi *radical* partition can; in English the name of this partition is *power* tessellation (diagram) [62]).

Thus, using the Voronoi–Delaunay method, it is necessary to specify which type of partition we use. In [15], the main calculations were performed using S-partition. In recent studies, for simplicity, we began to employ P-partition. Furthermore, to calculate the empty volumes of the boundary region and its parts (see below) we use P-partition since the calculation of the volumes of the intersection of Voronoi regions and Delaunay simplices was implemented only for the case of flat boundaries of Voronoi regions [49]. It is clear that the values of the volumes calculated using various types of Voronoi partition will be somewhat different. However, this is not so important for volumetric problems, where the dependence of these characteristics on temperature and pressure is of physical interest. (Note that for the calculation of the apparent volume by formula (7), it does not matter which type of Voronoi partition is used.)

INTRINSIC VOLUME AND CONTRIBUTION FROM SOLVENT

By the intrinsic volume of a molecule in solution V_{int} we propose to understand the volume of the Voronoi region of this molecule [12, 15, 63- 65]:

$$V_{int} = V_{Vor} = \sum v_m. \tag{10}$$
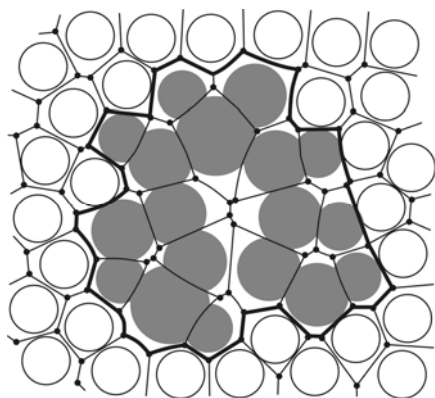
Fig. 10. Voronoi region of a polyatomic molecule. It is the sum of the Voronoi regions of all its atoms. The molecule is shown by dark disks, the solvent is shown by light disks, and the boundary of the region is shown by a bold solid line.

Fig. 11. Apparent volume V_{app} and its components V_{int} and ΔV for hIAPP (*a*) and Aβ_{42} (*b*) in water at different temperatures from [15].

In geometric terms, this is a region of space whose points are closer to the given molecule than to the solvent molecules (Fig. 10). The intrinsic volume of a molecule in solution includes its van der Waals volume, the volume of internal voids, and partly the volume of the empty space outside molecule, which is naturally associated with the molecule, rather than with the solvent.

Thus, the apparent volume V_{app} can be determined by any of the methods described above, and the intrinsic volume V_{int} is calculated as the Voronoi volume of the molecule. Thus, the contribution of the solvent can be found by the formula $\Delta V = V_{app} - V_{int}$.

Fig. 11 shows the temperature dependence of the apparent volume and its components (V_{int} and ΔV) for polypeptides hIAPP and Aβ_{42} [15]. They behave in a similar way, and the intrinsic volume is greater than the apparent volume at all temperatures. Thus, the contribution from the solvent is negative (the molecule compacts the nearest water). This contribution is about 10% of the apparent volume at low temperatures and decreases in magnitude under heating.

For solutions of noble gases, the apparent and intrinsic volumes also increase monotonically with temperature (Fig. 12). However, here the apparent volume is found to be greater than the intrinsic volume in a wide range of temperatures (except for the lowest ones, corresponding to supercooled water). This means that the surrounding water is less dense than that in the bulk. A small increase in the volume of a one-atom spherical molecule with temperature is due to the involvement of external voids, which increase in number due to a decrease in the density of water with temperature. The contribution of ΔV increases with temperature and is approximately 20% of the apparent volume at 350 K. This distinguishes solutions of noble gases and methane from solutions of large molecules. Note that in [42], we investigated solutions of methane and all noble gases (except helium). All of them show a similar behavior of volumetric parameters.

For the amphiphilic molecule C_8E_6, the situation is more complicated (Fig. 13). Here the apparent and intrinsic volumes also increase with temperature, but the contribution from the solvent changes sign. It is interesting that the change of sign correlates with the change in the hydrophobicity of this molecule [51]. Thus, the behavior of volumetric characteristics of the molecule reflects the thermodynamic and chemical properties of the solution. This is not surprising since the apparent volume itself is a thermodynamic characteristic.
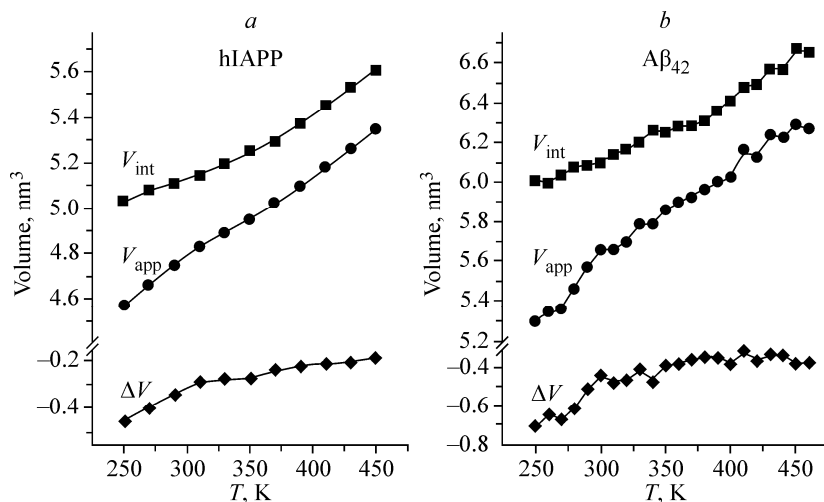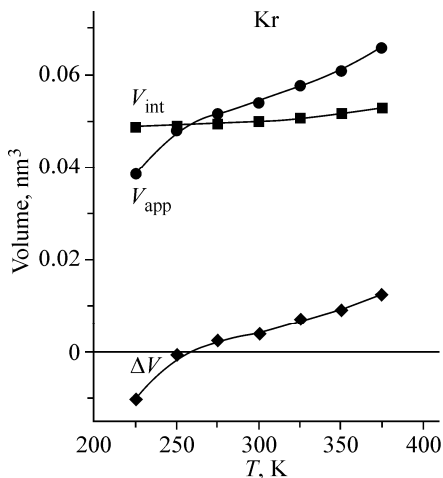
Fig. 12. Apparent volume and its components for a Kr atom in water at different temperatures, from [42].
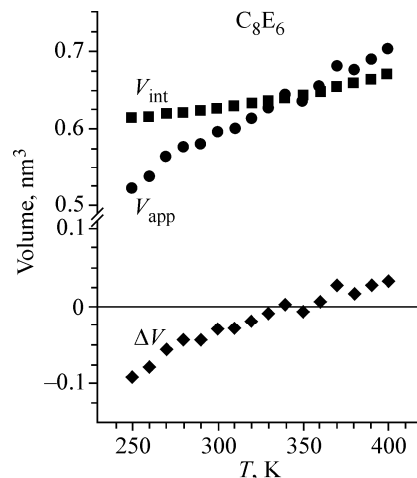
Fig. 13. Apparent volume and it is its components for a C_8E_6 molecule in water at different temperatures, from [51].

THERMAL VOLUME

By the thermal volume is meant the additional empty volume that arises in the contact area of the molecule with the solvent due to the nonoptimal mutual arrangement of the atoms of the molecule and the solvent [1, 16]. It is believed that this volume increases with temperature, and this increase is more rapid than that of the volume of the molecule. This contribution to the apparent volume can be identified and evaluated by studying computer models of solutions.

To study the boundary region between the molecule and solvent, it is proposed to invoke the Delaunay partition, in addition to the Voronoi partition [53, 54]. In our recent papers, we introduced the notion of *a Delaunay layer* [15, 66, 67]. Using Delaunay layers, it is possible to perform a decomposition of interatomic voids of the solution starting from the boundary layer, just as, using the Voronoi partition, we identify successive atomic shells (Voronoi shells) starting from the nearest neighbors of the solute molecule. In this case, we are interested in only one Delaunay layer, covering the spatial region between the molecule and the solution (Fig. 14).

It consists of Delaunay simplices whose vertices lie simultaneously on the atoms of the molecule and solvent. The mathematical properties of this layer are discussed in detail in our paper [66]. It is a solid shell of finite thickness which surrounds the molecule and covers the voids of the boundary layer.

We will call the empty volume of the Delaunay layer the *boundary* empty volume and denote it as V_B. (The empty volume is defined in the usual way as the difference between the volume of the Delaunay simplices that make up this layer and the volume occupied by parts of the atoms entering these simplexes.) This quantity can be used to characterize the thermal volume corresponding to this molecule. However, the quantity V_B should not be identified with the contribution V_T in formula (2). Figure 15 shows that our boundary volume V_B consists of two parts — one is associated with the molecule and the other with the solvent. In the first case, this is the empty volume of the intersection of our Delaunay simplices and Voronoi regions belonging to the atoms of the molecule ly — we denote it as V_B^M. In the second case, this is the empty volume of the intersection of the same simplices with the Voronoi regions of the solvent (V_B^S). The method of calculation of these volumes is described in [68].

Using selected region V_B^M, we can represent the intrinsic volume of the molecule V_{int} as

$$V_{int} = V_M + V_B^M,$$

(11)

S283
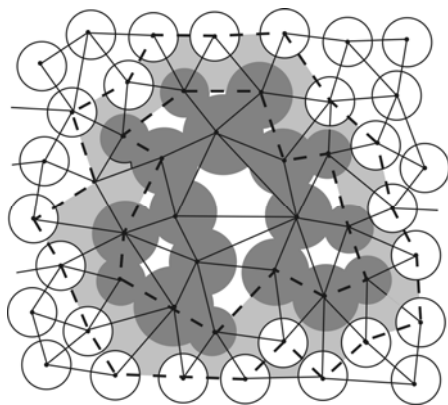
Fig. 14. Illustration of the Delaunay layer around a solute molecule (shown by dashed lines). It consists of Delaunay simplices (shown by thin lines) and covers the voids related to the boundary layer.
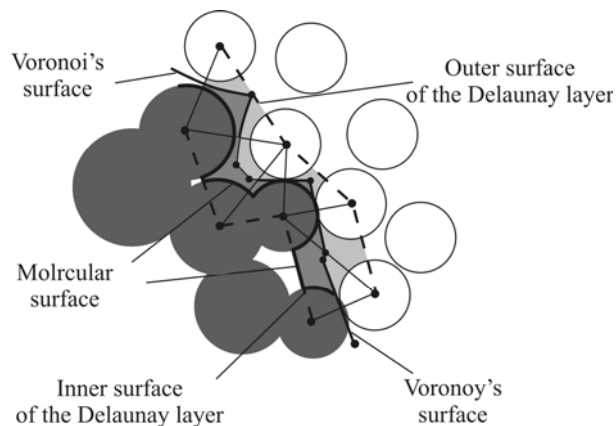
Fig. 15. Fragment of the boundary region of the solute molecule shown in Fig. 14. The dashed lines indicate the inner and outer surfaces of the Delaunay layer. The empty space of the layer defines the volume V_B. The solid thick line between the molecule and solution is the surface of the Voronoi region of the molecule and divides the Delaunay layer into the parts associated with the molecule and the solvent V_B^M and V_B^S. The solid line shows the boundary of the molecule. It consists of surface regions of the atoms and the faces of the Delaunay simplices covering the gaps between the atoms of the molecule.

where V_M is the molecular volume. It includes the van der Waals volume of the molecule and all internal voids. Its boundary is the surface of the atom and the faces of the Delaunay simplices which close the gaps between the atoms (Fig. 15). This method of determining the molecular volume is somewhat different from the well-known method of molecular biology using molecular surface, where there are gaps between the atoms are covered by the surface of a rolling probe sphere of a certain radius [22]. The question of which of the methods of determining V_M is more physical remains open. In the analysis of molecular dynamics models, we tend to prefer our method. It takes into account the actual, rather inhomogeneous, arrangement of water molecules around the solvent molecule, whereas the use of the Connolly surface [22] implies that water molecules are spread around our molecule with a uniform density.

Using (11), formula (1) can be written as

$$V_{app} = V_M + V_B^M + \Delta V. \tag{12}$$

Separation of the contribution V_M makes it possible to examine the changes occurring within the molecule, while the term V_B^M is responsible for the appearance of an additional empty space around the molecule.

Fig. 16 shows the temperature dependence of the apparent volume of a hIAPP molecule and its components. It can be seen that the increase in the apparent volume of the polypeptide molecule with temperature is mainly due to the boundary region (V_B^M), whereas the molecular volume V_M is practically unchanged. We can argue that the coefficient of thermal expansion of the apparent volume of the IAPP molecule is determined by the thermal volume, although the contribution V_B^M, obviously, does not represent it completely.

Fig. 17 explains how this occurs. As the temperature increases, the density of water decreases and the volume of intermolecular voids increases, resulting in an increase in the Voronoi volume of the molecule. However, the molecule itself may remain unchanged.
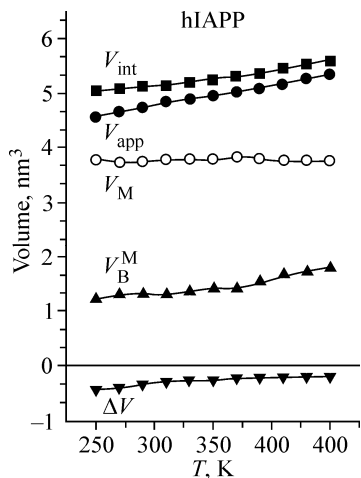
Fig. 16. Apparent volume of a hIAPP molecule and its components versus temperature [67].
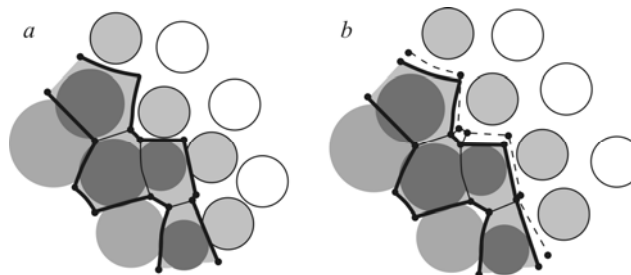
Fig. 17. Fragment of the boundary region the molecule in the solution (*a*). The thick solid line shows the boundary of the Voronoi region. The same fragment, but the density of the solvent is lower (*b*). The dotted line shows the new boundary between the molecule and the solvent.
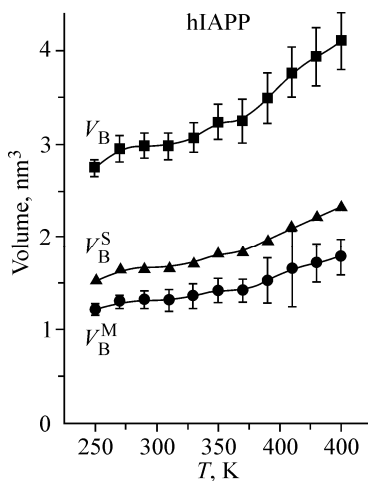
Fig. 18. Empty boundary volume V_B and its components V_B^M and V_B^S around a hIAPP molecule versus temperature.

Fig. 18 shows the variation of the entire empty boundary volume V_B with temperature. It can be seen that it increases by approximately 30% in this range of temperatures, whereas the density of pure water changes by only about 10% [15, 36]. This means that the packing in the boundary region is substantially more sensitive to changes in temperature than that in bulk water.

Note that the part V_B^S is not a component of the apparent volume, unlike V_B^M. It is associated with the solvent (hydrate shell) and should therefore be taken into account in the apparent volume after deducting from it the fraction of the volume corresponding to these molecules in pure water. However, it is not clear how to separate the part associated with pure water from the volume V_B^S.

CONCLUSIONS

In this paper, we have shown how to extract volumetric characteristics from a computer model of solutions. Dilute solutions of simple and complex molecules (one solute molecule in the simulation box, surrounded by a large number of water molecules) have been studied. It has been shown how to calculate the partial molar volume (in this case, it coincides with the apparent volume of the molecule) and its components associated with the molecule, the boundary layer, and the solvent.

Different methods for calculating the apparent volume have been considered. In *the direct* method, the difference between the average volumes of the simulation box with the solution and the same amount of the pure solvent is found explicitly. This is the simplest method, but obtaining reliable results requires careful averaging of the volumes of simulation boxes. In *local* methods, only the neighborhood of the solute molecule is used. In the simplest case, this approach is equivalent to the well-known method of calculating the partial molar volume using the Kirkwood-Buff integral. A modification of the local method is discussed, in which the volume of the environment of the molecule is calculated as the sum of the Voronoi regions of all atoms in this environment. This combined approach is more reliable than the traditional one.

To identify the components of the apparent volume, it is proposed to use the Delaunay–Voronoi partition, which provides a convenient tool for calculating volumetric quantities. The volume of the *Voronoi region of a solute molecule* in solution is suggested to be used as *the intrinsic* volume of the molecule. It includes the van der Waals volume of the molecule, all internal voids, and the part of the intermolecular empty space that is naturally associated with the molecule.

It is thought that the boundary region between the molecule and solvent plays an important role in changing the partial molar volume with temperature. To identify and analyze this region, it is proposed to use a *Delaunay layer* consisting of Delaunay simplices whose vertices are simultaneously on the atoms of the solute molecule and the solvent. Considering the intersections of the boundary Voronoi shells and the Delaunay layer, the empty boundary volume can be divided into the part relating to the molecule and the part relating to the solution. It has been found that the universal increase in the apparent volume with temperature for large molecules is mainly due to an increase in the volume of voids in the boundary layer under heating, i.e., due to the *thermal* volume.

For large molecules (polypeptides), the solvent gives a negative contribution to the apparent volume for all temperatures studied. In contrast, for simple hydrophobic molecules (methane, noble gas atoms), the contribution from the solvent is positive (except in the region of supercooled water). For a molecule of surfactant (C_8E_6), the contribution from the solution with increasing temperature changes sign (from positive to negative), which correlates with the change in the hydrophobicity of the molecule.

REFERENCES

1. T. V. Chalikian, *Annu. Rev. Biophys. Biomol. Struct*., **32**, 207-235 (2003).
2. L. Mitra, N. Smolin, R. Ravindra, C. Royer, and R. Winter, *Phys. Chem. Chem. Phys*., **8**, 1249-1265 (2006).
3. K. Akasaka, A. R. Latif, A. Nakamura, K. Matsuo, H. Tachibana, and K. Gekko, *Biochemistry*, **46**, 10444-10450 (2007).
4. R. Ravindra, C. Royer, and R. Winter, *Phys. Chem. Chem. Phys*., **6**, 1952-1961 (2004).
5. R. Filfil and T. V. Chalikian, *J. Mol. Biol*., **299**, 827-842 (2000).
6. J. Rösgen and H. J. Hinz, *Biophys. Chem*., **83**, 61-71 (2000).
7. M. Haeckel, H.-J. Hinza, and G. R . Hedwig, *Biophys. Chem*., **82**, 35-50 (1999).
8. T. Kamiyama and K. Gekko, *Chem. Lett*., **10**, 1063/1064 (1997).
9. T. V. Chalikian, M. Totrov, T. Abagyan, and K. J. Breslauer, *J. Mol. Biol*., **260**, 588-603 (1996).

10. E. A. Moelwyn-Hughes, *Physical Chemistry*, *Book 2*, Izd. Inostr. Lit., Moscow (1962).

11. A. Yu. Tsivadze (ed.), in: *Theoretical and Experimental Methods of Solution Chemistry*, (*Problems of Solution Chemistry*), Chapter 8, *Densitometry of Solutions*, 425-463, Prospekt, Moscow (2011).

12. M. Marchi, *J. Phys. Chem. B*, **107**, 6598-6602 (2003).

13. C. Klofutar, J. Horvat, and D. Rudan-Tasič, *Acta Chim. Slov.*, **53**, 274-283 (2006).

14. I. Brovchenko, R. R. Burri, A. Krukau, A. Oleinikova, and R. Winter, *J. Chem. Phys.*, **129**, 195101 (2008).

15. V. P. Voloshin, N. N. Medvedev, M. N. Andrews, R. R. Burri, R. Winter, and A. Geiger, *J. Phys. Chem. B*, **115**, 14217-14228 (2011).

16. T, Imai *Cond. Matter Phys.*, **10**, No. 3(51), 343-361 (2007).

17. R. A. Pierotti, *J. Phys. Chem.*, **69**, 281-288 (1965).

18. D. P. Kharakoz, *J. Solut. Chem.*, **21**, 569 (1992).

19. H. Reiss, H. L. Frisch, and J. L. Lebowitz, *J. Chem. Phys.*, **31**, 369 (1959).

20. F. H. Stillinger, *J. Solut. Chem.*, **2**, 141 (1973).

21. F. M. Richards, *Methods Enzymol.*, **115**, 440-646 (1985).

22. M. J. Connolly, *J. Appl. Crystallogr.*, **16**, 548-558 (1983).

23. M. L. Connolly, *J. Am. Chem. Soc.*, **107**, 1118-1124 (1985).

24. J. Liang, H. Edelsbrunner, P. Fu, P. V. Sudhakar, and S. Subramaniam, *Proteins: Struct. Funct. Genet.*, **33**, 1-17 (1998).

25. N. Patel, D. N. Dubins, R. Pomes, and T. V. Chalikian, *J. Phys. Chem. B*, **115**, 4856-4862 (2011).

26. T. Imai, A. Kovalenko, and F. Hirata, *J. Phys. Chem. B*, **109**, 6658-6665 (2005).

27. J. G. Kirkwood and F. P. Buff, *J. Chem. Phys.*, **19**, 774 (1951).

28. A. Ben-Naim, *Molecular Theory of Solutions*, Oxford University Press, Oxford (2006).

29. N. Matubayas and R. M. Levy, *J. Phys. Chem.*, **100**, 2681-2688 (1996).

30. M. S. Moghaddam and Hue Sun Chan., *J. Chem. Phys.*, **126**, 114507 (2007).

31. A. V. Sangwai and H. S. Ashbaugh, *Ind. Eng. Chem. Res.*, **47**, 5169-5174 (2008).

32. D. Chandler, *J. Chem. Phys.*, **59**, 2742-2747 (1973).

33. J.-P. Hansen, and I. R. McDonald, *Theory of Simple Liquids*, 3rd ed., Academic Press, London (2006).

34. Song-Ho Chong and F. Hirata, *J. Phys. Chem. B*, **101**, 3209-3220 (1997).

35. T. Imai, M. Kinoshita, and F. Hirata, *J. Chem. Phys.*, **112**, 9469 (2000).

36. I. Brovchenko, M. N. Andrews, and A. Oleinikova, *Phys. Chem. Chem. Phys.*, **12**, 4233-4238 (2010).

37. I. Yu, T. Tasaki, K. Nakada, and M. Nagaoka, *J. Phys. Chem. B*, **114**, 12392-12397 (2010).

38. H. S. Ashbaugh, L. Liu, and L. N. Surampudi, *J. Chem. Phys.*, **135**, 054510 (2011).

39. A. C. Moskalev, *Bachelor's Diploma: Investigation of Hydration Shells of Molecules of Noble Gases in Aqueous Solutions*, Novosibirsk State University (2012).

40. M. N. Andrews and R. Winter, *Biophys. Chem.*, **156**, 43-50 (2011).

41. N. V. Plyasunova, A. V. Plyasunov, and E. L. Shock, *Intern. J. Thermophys.*, **25**, 351-360 (2004).

42. A. S. Moskalev, A. V. Anikeenko, N. N. Medvedev, and A. Geiger, *Book of Abstracts. EMLG-JMLG Annual Meeting* (2013).

43. J. L. F. Abascal and C. Vega, *J. Chem. Phys.*, **123**, 234505 (2005).

44. H. L. Pi, J. L. Aragones, C. Vega, E. G . Noya, J. L. F. Abascal, M. A. Gonzalez, and C. McBride, *Mol. Phys.*, **107**, 365-374 (2009).

45. S. K. Pal, J. Peon, and A. H. Zewail, *PNAS*, **99**, 1763-1768 (2002).

46. A. Ben-Naim, *J. Chem. Phys.*, **128**, 234501 (2008).

47. F. Hirata, *Molecular Theory of Solvation* (*Understanding Chemical Reactivity*), Kluwer Academic Publishers, Boston (2003).

48. J. Liang, *Computational Methods for Protein Structure Prediction and Modeling. Biological and Medical Physics Biomedical Engineering*, Springer, New York (2007), pp. 181-206.

49. V. P. Voloshin, A. V. Anikeenko, N. N. Medvedev, and A. Geiger, *Proc. 9th Int. Symp. on Voronoi Diagrams in Science and Engineering* (ISVD 2011), June 28th-30th, Qingdao, China (2011), pp. 170-176.

50. F. Cazals, H. Kanhere, and S. Loriot, *ACM Trans. Math. Softw*. (2011), p. 3.

51. A. V. Kim, N. N. Medvedev, and A. Geiger, *J. Mol. Liq*., **189**, 74-80 (2013).

52. *Computational Geometry Algorithms Library* (*CGAL*). http://www.cgal.org

53. A. Okabe, B. Boots, K. Sugihara, and S. Chiu, *Spatial Tessellations — Concepts and Applications of Voronoi Diagrams*. Wiley, New York (2000).

54. N. N. Medvedev, *Voronoi–Delaunay Method in Studies of Non-Crystalline Systems*, Izd. SO RAN, Novosibirsk (2000).

55. V. P. Voloshin, A. V. Anikeenko, N. N. Medvedev, A. Geiger, and D. Stoyan, *Proc.7th Int. Symp. on Voronoi Diagrams in Science and Engineering*, Quebec, 28-30. Quebec, Canada (2010), pp. 254-259.

56. G. F. Voronoi, *J. Reine Angew Math*., **136**, 67 (1909).

57. B. N. Delaunay, *Proc. Int. Math. Congress*, Toronto, August 11-16 (1924); University of Toronto, Press: Toronto (1928); pp. 695-700.

58. S. V. Anishchik and N. N. Medvedev, *Phys. Rev. Lett*., **75**, 4314-4317 (1995).

59. M. G. Alinchenko, A. V. Anikeenko, N. N. Medvedev, V. P. Voloshin, M. Mezei, and P. Jedlovszky, *J. Phys. Chem. B*, **108**, 19056-19067 (2004).

60. N. N. Medvedev, V. P. Voloshin, V. A. Luchnikov, and M. L. Gavrilova, *J. Comput. Chem*., **27**, 1676-1692 (2006).

61. D.-S. Kim, Y. Cho, and K. Sugihara, *Computer-Aided Design*, **42**, No. 10, 874-888 (2010).

62. F. Aurenhammer, *SIAM J. Comput*., **16**, 78-96 (1987).

63. P. Procacci and R. Scateni, *Int. J. Quantum Chem*., **42**, 1515-1528 (1992).

64. E. Paci and M. Marchi, *PNAS*, **93**, 11609-11614 (1996).

65. V. Lounnas and B. M. Pettitt, *Proteins: Struct., Funct., Genet*., **18**, 133-147 (1994).

66. A. V. Kim, V. P. Voloshin, N. N. Medvedev, and A. Geiger, *Proc. Int. Symp. on Voronoi Diagrams in Science and Engineering,* Rutgers University, USA. June 27-29, 2012, p. 95-102.

67. A. V. Kim, V. P. Voloshin, N. N. Medvedev, and A. Geiger, *Trans. Comp. Sci. J.*, Springer (2013).

68. V. P. Voloshin and N. N. Medvedev, *Proc. Int. Symp. on Voronoi Diagrams in Science and Enginering*, St. Petersburg, Russia, July 8-10 (2013) (in preparation).